

Decay behaviors of the P_c hadronic molecules

Yong-Hui Lin^{1,2,*}, Chao-Wei Shen^{1,2,†}, Feng-Kun Guo^{1,2,‡} and Bing-Song Zou^{1,2,§}

¹*CAS Key Laboratory of Theoretical Physics, Institute of Theoretical Physics,
Chinese Academy of Sciences, Beijing 100190, China*

²*School of Physical Sciences, University of Chinese Academy of Sciences, Beijing 100049, China*

July 3, 2018

Abstract

The $P_c(4380)$ and $P_c(4450)$ states observed recently by LHCb experiment were proposed to be either $\bar{D}\Sigma_c^*$ or $\bar{D}^*\Sigma_c$ S-wave bound states of spin parity $J^P = \frac{3}{2}^-$. We analyze the decay behaviors of such two types of hadronic molecules within the effective Lagrangian framework. With branching ratios of ten possible decay channels calculated, it is found that the two types of hadronic molecules have distinguishable decay patterns. While the $\bar{D}\Sigma_c^*$ molecule decays dominantly to $\bar{D}^*\Lambda_c$ channel with a branching ratio by 2 orders of magnitude larger than to $\bar{D}\Lambda_c$, the $\bar{D}^*\Sigma_c$ molecule decays to these two channels with a difference of less than a factor of 2. Our results show that the total decay width of $P_c(4380)$ as the spin-parity- $\frac{3}{2}^-$ $\bar{D}\Sigma_c^*$ molecule is about a factor of 2 larger than the corresponding value for the $\bar{D}^*\Sigma_c$ molecule. It suggests that the assignment of $\bar{D}\Sigma_c^*$ molecule for $P_c(4380)$ is more favorable than the $\bar{D}^*\Sigma_c$ molecule. In addition, $P_c(4450)$ seems to be a $\bar{D}^*\Sigma_c$ molecule with $J^P = \frac{5}{2}^+$ in our scheme. Based on these partial decay widths of $P_c(4380)$, we estimate the cross sections for the reactions $\gamma p \rightarrow J/\psi p$ and $\pi p \rightarrow J/\psi p$ through the s-channel $P_c(4380)$ state. The forthcoming γp experiment at JLAB and πp experiment at JPARC should be able to pin down the nature of these P_c states.

*Email address: linyonghui@itp.ac.cn

†Email address: shencw@itp.ac.cn

‡Email address: fkguo@itp.ac.cn

§Email address: zoubs@itp.ac.cn

1 Introduction

In recent years, a large number of new hadrons were discovered experimentally following the developments in the high-energy experiments and the accumulation of the precise data in the low-energy exclusive measurements [1]. Some of these hadrons were suggested to have internal structure more complex than the simple $q\bar{q}$ configuration for mesons or qqq configuration for baryons in the traditional picture of the constituent quark models, and are good candidates of exotic hadrons. Study of exotic hadrons has become a central topic of hadron spectroscopy in the past decade (for a recent review, see Ref. [2]). Especially, the observation of two hidden charm pentaquark-like structures, $P_c^+(4380)$ and $P_c^+(4450)$, by the LHCb Collaboration [3] attracts much attention. The existence of relatively narrow hidden-charm pentaquarks has been suggested and their masses have been predicted in Refs. [4–7]. The P_c structures are observed in the $J/\psi p$ invariant mass distribution in the process of $\Lambda_b^0 \rightarrow J/\psi p K^-$ decay. Assuming they are resonances, the reported mass and width of the $P_c^+(4380)$ are $(4380 \pm 8 \pm 29)$ MeV and $(205 \pm 18 \pm 86)$ MeV, respectively, while the $P_c^+(4450)$ has a mass of $(4449.8 \pm 1.7 \pm 2.5)$ MeV and a width of $(39 \pm 5 \pm 19)$ MeV. The spin-parities of these two P_c states are not well determined yet. According to experimental analyses, the most favorable set of the spin and parity for the lower and the higher peaks is $J^P = (3/2^-, 5/2^+)$.

Many models for the structure and production of P_c states have been proposed, such as the baryon–meson molecules [8–15], compact pentaquark states [16–22] and baryocharmonia [23], while the possibility of rescattering-induced kinematical effects has also been discussed [24–27]. Some of these models are used to predict other possible pentaquark-like hadrons, and others are built to explore the internal structure of the P_c states. Among them, the one which we are interested in is that the $P_c(4380)$ and $P_c(4450)$ are interpreted as the hadronic molecular states composed of either $\bar{D}\Sigma_c^*(2520)$ or $\bar{D}^*\Sigma_c(2455)$ since their masses are quite close to these two thresholds. Based on this hadronic molecular picture, we try to analyze the decay behaviors of P_c states by calculating the partial widths of the P_c states into some possible final states in the framework of effective Lagrangian approach. It will help us to distinguish different interpretations about the structure of P_c states and can be examined by future experiments.

This work is organized as follows. After introduction, we first present the details of the theoretical formalism in Sec. 2. The predicted decay properties and some discussion are presented in Sec. 3. Finally, a brief summary will be given and an appendix is presented in the end.

2 Formalism

In this section, we present the fundamental formalism for the investigation about the decay properties of the P_c states in the $\bar{D}\Sigma_c^*$ and $\bar{D}^*\Sigma_c$ molecular pictures. The spin-parity of $P_c(4380)$ state is set to be $\frac{3}{2}^-$ in the whole work.

Since both the Σ_c^{*+} and Σ_c^{*++} are unstable with a width of about 15 MeV, and decays dominantly into the $\pi\Lambda_c$, a natural decay mode for the $\bar{D}\Sigma_c^*$ molecule would be the three-body $\bar{D}\pi\Lambda_c$, as shown in Fig. 1, where final state interaction has been neglected. The decay widths of D^* and Σ_c are less than 2 MeV. Therefore, the three- and four-body decays through the decays of the D^* and Σ_c in the $\bar{D}^*\Sigma_c$ hadronic molecule can be neglected.

Because of the small widths of the Σ_c and Σ_c^* , these three-body decay modes are not the main contribution to the total width of the hadronic molecules under consideration. The P_c states can also decay into a meson and a baryon. The two-body decay modes which will be considered in this paper are listed in Table 1. Note that the threshold of $\bar{D}\Sigma_c^*$ system is about 4386 MeV, 6 MeV higher than the central value of the mass of $P_c(4380)$. Thus, the $\bar{D}\Sigma_c^*$ channel appears only in the $P_c(4450)$ decay as shown in the table. One sees that some of the decays happen at relatively long distances, i.e., the involved momentum exchange is small, such as the ones into a pair of anti-charm meson and charm baryon. In principal, the partial widths of such decays could be calculated in the framework of a nonrelativistic effective field theory. However, due to the lack of knowledge of the interaction between the anti-charm mesons and charm baryons, we have to

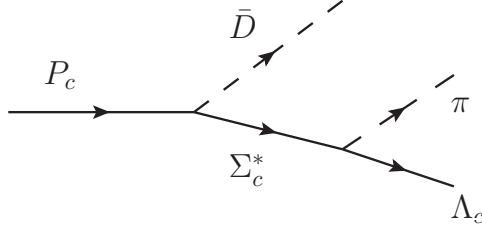


Figure 1: The three-body decay of the P_c state as the $\bar{D}\Sigma_c^*$ molecule.

Table 1: All possible final states for the $P_c(4380)$ and $P_c(4450)$ decay with $J^P = \frac{3}{2}^-$.

Initial state	Final states
$P_c(4380)(\bar{D}\Sigma_c^*)$	$\bar{D}^*\Lambda_c, J/\psi p, \bar{D}\Lambda_c, \pi N, \chi_{c0}p, \eta_c p, \rho N, \omega p, \bar{D}\Sigma_c$
$P_c(4380)(\bar{D}^*\Sigma_c)$	$\bar{D}^*\Lambda_c, J/\psi p, \bar{D}\Lambda_c, \pi N, \chi_{c0}p, \eta_c p, \rho N, \omega p, \bar{D}\Sigma_c$
$P_c(4450)(\bar{D}^*\Sigma_c)$	$\bar{D}^*\Lambda_c, J/\psi p, \bar{D}\Lambda_c, \pi N, \chi_{c0}p, \eta_c p, \rho N, \omega p, \bar{D}\Sigma_c, \bar{D}\Sigma_c^*$

rely on models such as exchanging the ρ meson in addition to the lightest pion. The decays into a pair of light meson and light baryon take place at short distances, and again an estimate of such decays can only be done in models. The triangle diagrams for the meson-exchange model of the two-body decays of the $\bar{D}\Sigma_c^*$ and $\bar{D}^*\Sigma_c$ hadronic molecules are shown in Fig. 2 and Fig. 3, respectively.

It should be mentioned that the sets of spin and parity for (\bar{D}, Σ_c^*) and (\bar{D}^*, Σ_c) are $(0^-, \frac{3}{2}^+)$ and $(1^-, \frac{1}{2}^+)$, respectively. Thus the P_c states of spin-parity $\frac{3}{2}^-$ may be considered as S -wave bound states of $\bar{D}\Sigma_c^*$ or $\bar{D}^*\Sigma_c$. Subject to the Lorentz covariant orbital-spin scheme [28], the S -wave couplings for the P_c with $J^P = \frac{3}{2}^-$ with the meson-baryon pairs of interest are given by

$$\begin{aligned}
\mathcal{L}_{\bar{D}\Sigma_c^*P_c} &= g_{\bar{D}\Sigma_c^*P_c} \bar{\Sigma}_c^{*\mu} P_{c\mu} \bar{D} + H.c., \\
\mathcal{L}_{\bar{D}^*\Sigma_cP_c} &= g_{\bar{D}^*\Sigma_cP_c} \bar{\Sigma}_c P_{c\mu} \bar{D}^{*\mu} + H.c.,
\end{aligned} \tag{1}$$

where two S -wave coupling constants $g_{\bar{D}\Sigma_c^*P_c}$ and $g_{\bar{D}^*\Sigma_cP_c}$ can be estimated by using [29, 30]

$$g^2 = \frac{4\pi}{4Mm_2} \frac{(m_1 + m_2)^{5/2}}{(m_1 m_2)^{1/2}} \sqrt{32\epsilon}, \tag{2}$$

here M , m_1 and m_2 denote the masses of the P_c state, $\bar{D}(\bar{D}^*)$ and $\Sigma_c(\Sigma_c^*)$, respectively, and ϵ is the binding energy. The factor $\frac{1}{4Mm_2}$ in Eq. (2) is introduced for the normalization of two fermion fields, P_c and $\Sigma_c(\Sigma_c^*)$. Assuming the physical state in question to be a pure S -wave hadronic molecule, the relative uncertainty of the above approximation for the coupling constant is $\sqrt{2\mu\epsilon}r$ where $\mu = m_1 m_2 / (m_1 + m_2)$ is the reduced mass of the bound particles, and r is the range of forces which may be estimated by the inverse of the mass of the particle that can be exchanged. Thus, for the $\bar{D}\Sigma_c^*$ and $\bar{D}^*\Sigma_c$ systems, r may be estimated as $1/m_\rho$ and $1/m_\pi$, respectively.

Besides the vertex described as Eq. (1) introduced in the previous discussion, the following effective Lagrangian [8, 9, 31–34] need to be presented for evaluating the decay amplitudes of the

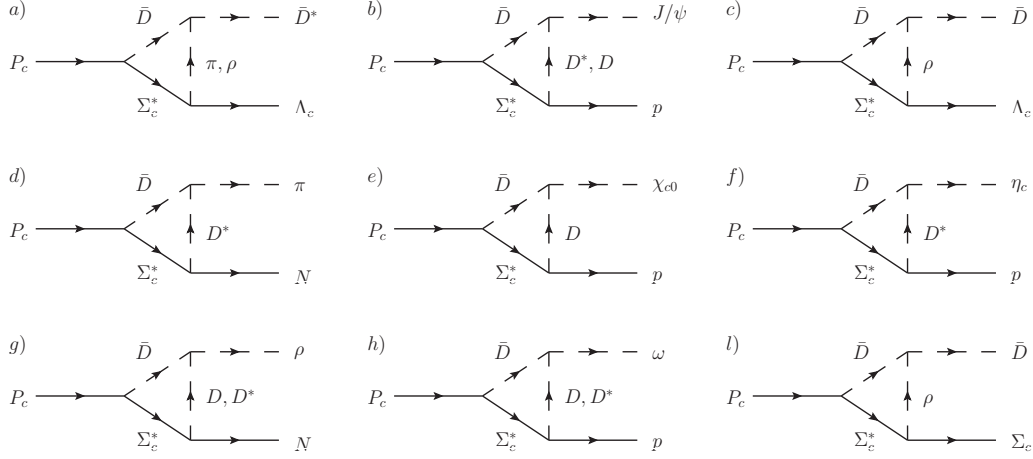


Figure 2: The decays of the P_c state as a $\bar{D}\Sigma_c^*$ molecule. a) $\bar{D}^*\Lambda_c$ channel with π exchange dominant and ρ exchange secondary. b) $J/\psi p$ channel with D^* exchange dominant and D exchange secondary. c) $\bar{D}\Lambda_c$ channel with ρ exchange. d) πN channel with D^* exchange. e) $\chi_{c0}p$ channel with D exchange. f) $\eta_{c0}p$ channel with D^* exchange. g) ρN channel with D exchange dominant and D^* exchange secondary. h) ωp channel with D exchange dominant and D^* exchange secondary. l) $\bar{D}\Sigma_c$ channel with ρ exchange.

Feynman diagrams shown in Fig. 1, 2, 3,

$$\mathcal{L}_{VP_1P_2} = ig_{VP_1P_2} (V_\mu \partial^\mu P_1 P_2 - V_\mu \partial^\mu P_2 P_1), \quad (3)$$

$$\mathcal{L}_{V_1V_2P} = -g_{V_1V_2P} \varepsilon^{\mu\nu\alpha\beta} (\partial_\mu V_{1\nu} \partial_\alpha V_{2\beta}) P, \quad (4)$$

$$\begin{aligned} \mathcal{L}_{V_1V_2V_3} = & -ig_{V_1V_2V_3} \left\{ V_1^\mu (\partial_\mu V_2^\nu V_{3\nu} - V_2^\nu \partial_\mu V_{3\nu}) + (\partial_\mu V_{1\nu} V_2^\nu - V_{1\nu} \partial_\mu V_2^\nu) V_3^\mu \right. \\ & \left. + V_2^\mu (V_{1\nu} \partial_\mu V_{3\nu} - \partial_\mu V_{1\nu} V_3^\nu) \right\}, \end{aligned} \quad (5)$$

$$\mathcal{L}_{PB_1B_2} = -ig_{PB_1B_2} \bar{B}_1 \gamma_5 B_2 P + H.c., \quad (6)$$

$$\mathcal{L}_{VB_1B_2} = g_{PB_1B_2} \bar{B}_1 \gamma_\mu V^\mu B_2 + H.c., \quad (7)$$

$$\mathcal{L}_{PBB^*} = g_{PBB^*} \bar{B}^{*\mu} \partial_\mu P B + H.c., \quad (8)$$

$$\mathcal{L}_{VBB^*} = -ig_{VBB^*} \bar{B}^{*\mu} \gamma^\nu \gamma_5 [\partial_\mu V_\nu - \partial_\nu V_\mu] B + H.c., \quad (9)$$

$$\mathcal{L}_{DD\chi_{c0}} = ig_{DD\chi_{c0}} DD + H.c., \quad (10)$$

$$\mathcal{L}_{D^*D^*\chi_{c0}} = ig_{D^*D^*\chi_{c0}} D^{*\mu} D_\mu^{*\dagger} + H.c., \quad (11)$$

where VP_1P_2 denotes $D^*D\pi$, $D^*D\eta_c$, ρDD , $J/\psi DD$ or ωDD , V_1V_2P denotes ρD^*D , ωD^*D , $J/\psi D^*D$, $D^*D^*\pi$ or $D^*D^*\eta_c$, $V_1V_2V_3$ denotes $D^*D^*\rho$, $D^*D^*\omega$ or D^*D^*J/ψ , PB_1B_2 denotes $DN\Sigma_c$, $\pi\Sigma_c\Sigma_c$ or $\pi\Sigma_c\Lambda_c$, VB_1B_2 means $\rho\Sigma_c\Lambda_c$, $\rho\Sigma_c\Sigma_c$ or $D^*N\Sigma_c$, PBB^* means $\pi\Lambda_c\Sigma_c^*$ or $DN\Sigma_c^*$, and finally VBB^* denotes $\rho\Sigma_c\Sigma_c^*$, $\rho\Lambda_c\Sigma_c^*$ or $D^*N\Sigma_c^*$. Another essential part in studying the decay properties of a hadronic molecule is to estimate the coupling constants appearing in related vertices. The values of coupling constants $g_{D^*D\pi}$, $g_{\pi\Sigma_c\Lambda_c}$ and $g_{\pi\Lambda_c\Sigma_c^*}$ are deduced from the precise experimental data of the decay widths of D^* , Σ_c and Σ_c^* . In the heavy quark limit, the S -wave heavy mesons D and D^* are in the same spin multiplet. As a result, $g_{D^*D^*\pi}$ and $g_{D^*D\pi}$ are related to each other in that limit up to a normalization factor. We will take $g_{D^*D^*\pi} = \bar{M}_D g_{D^*D\pi}/2$ with \bar{M}_D the average mass of D and D^* mesons following Ref. [33]. In addition, in the same limit there exist relations: $g_{D^*D\eta_c} = g_2 \sqrt{m_{\eta_c}} m_D$, $g_{D^*D^*\eta_c} = g_2 \sqrt{m_{\eta_c}}$, $g_{DD\chi_{c0}} = -\sqrt{3} g_1 \sqrt{m_{\chi_{c0}}} m_D$, and $g_{D^*D^*\chi_{c0}} = -\frac{1}{\sqrt{3}} g_1 \sqrt{m_{\chi_{c0}}} m_{D^*}$. However, because all of the ground state S -wave and P -wave charmonia are below open-charm thresholds, neither g_1 nor g_2 can be measured directly. For the numerical estimate of the partial widths, we will take the model values $g_1 = -4 \text{ GeV}^{-1/2}$ and

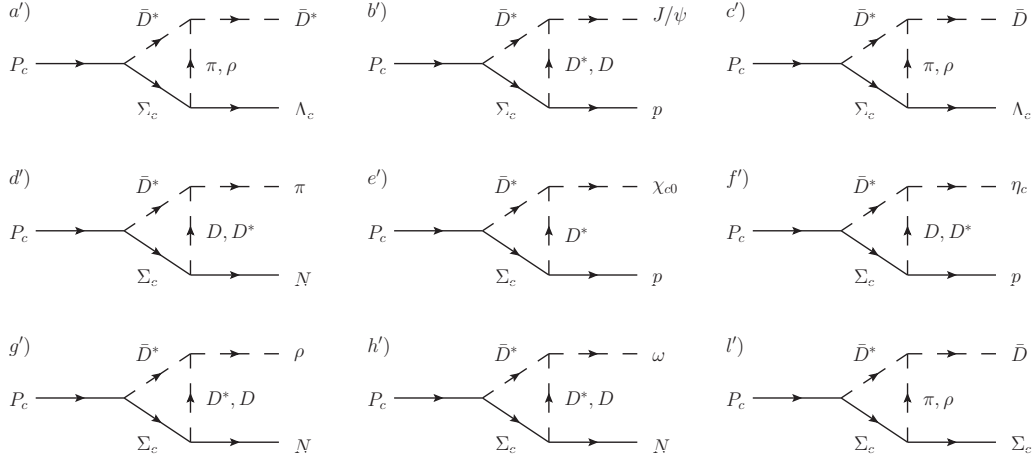


Figure 3: The decays of the P_c state as the $\bar{D}^*\Sigma_c$ molecule. $a')$ $\bar{D}^*\Lambda_c$ channel with π exchange dominant and ρ exchange secondary. $b')$ $J/\psi p$ channel with D^* exchange dominant and D exchange secondary. $c')$ $\bar{D}^*\Lambda_c$ channel with π exchange dominant and ρ exchange secondary. $d')$ πN channel with D exchange dominant and D^* exchange secondary. $e')$ $\chi_{c0} p$ channel with D^* exchange. $f')$ $\eta_c p$ channel with D exchange dominant and D^* exchange secondary. $g')$ ρN channel with D^* exchange dominant and D exchange secondary. $h')$ ωp channel with D^* exchange dominant and D exchange secondary. $i')$ $\bar{D}^*\Sigma_c$ channel with π exchange dominant and ρ exchange secondary.

$g_2 = 2.36 \text{ GeV}^{-3/2}$ [35].¹ The following coupling constants are taken from Ref. [36]: $g_{D^*D^*J/\psi} = g_{J/\psi DD} = 7.64$, $g_{D^*D^*\rho} = g_{\rho DD} = 2.52$, $g_{D^*D^*\omega} = g_{\omega DD} = -2.84$. The other coupling constants used in our work are listed in Table. 2. One should notice that most of the these values can only regarded as a rough estimate, which should suffice for an order-of-magnitude estimate of the decay rates under consideration.

Table 2: The coupling constants used in this paper from Refs. [8, 9, 37, 38].

Coupling constants	$g_{D^*D\pi}$	$\frac{g_{D^*D^*\pi}}{(\text{GeV}^{-1})}$	$g_{\pi\Sigma_c\Lambda_c}$	$\frac{g_{\pi\Lambda_c\Sigma_c^*}}{(\text{GeV}^{-1})}$	$\frac{g_{\rho D^*D}}{(\text{GeV}^{-1})}$	$\frac{g_{\omega D^*D}}{(\text{GeV}^{-1})}$	$\frac{g_{J/\psi D^*D}}{(\text{GeV}^{-1})}$	$g_{DN\Sigma_c}$
Value	8.4	8.65	19.3	7.46	2.82	-3.18	8.64	2.69
Coupling constants	$g_{\pi\Sigma_c\Sigma_c}$	$g_{D^*N\Sigma_c}$	$g_{\rho\Sigma_c\Lambda_c}$	$g_{\rho\Sigma_c\Sigma_c}$	$\frac{g_{DN\Sigma_c^*}}{(\text{GeV}^{-1})}$	$\frac{g_{D^*N\Sigma_c^*}}{(\text{GeV}^{-1})}$	$\frac{g_{\rho\Lambda_c\Sigma_c^*}}{(\text{GeV}^{-1})}$	$\frac{g_{\rho\Sigma_c\Sigma_c^*}}{(\text{GeV}^{-1})}$
Value	10.76	3.0	-1.04	13.8	6.5	2.92	10	5.77

In the rest frame of the initial state, the two-body decay width can be written as

$$d\Gamma = \frac{F_I}{32\pi^2} \overline{|\mathcal{M}|^2} \frac{|\mathbf{p}_1|}{M^2} d\Omega, \quad (12)$$

where $d\Omega = d\phi_1 d(\cos\theta_1)$ is the solid angle of particle 1, M is the mass of the P_c , the factor F_I from the isospin symmetry is a constant for a certain channel, and the polarization-averaged squared amplitude $\overline{|\mathcal{M}|^2}$ means $\frac{1}{4} \sum_{\text{spin}} |\mathcal{M}|^2$. The amplitude expressions for all of the processes shown in Figs. 2 and 3 are collected in the Appendix.

Among all the triangle diagrams, some of the amplitudes, corresponding to the exchange of a pseudoscalar meson for the D -wave decay modes [9, 39], are ultraviolet (UV) finite while the others diverge. Nevertheless, even the UV finite loops receive short-distance contributions if we integrate over the whole momentum space. We will employ the following UV regulator which suppress

¹Note that these values are half of those in Ref. [35] due to the difference in conventions.

short-distance contributions and thus can render all the amplitudes UV finite [8, 9, 40, 41]

$$\tilde{\Phi}(p_E^2/\Lambda_0^2) \equiv \exp(-p_E^2/\Lambda_0^2), \quad (13)$$

where p_E is the Euclidean Jacobi momentum, and the cutoff Λ_0 denotes a hard momentum scale which suppresses the contribution of the two constituents at short distances $\sim 1/\Lambda_0$. The value of Λ_0 should be much larger than the typical momentum in the bound state, given by $\sqrt{2\mu\epsilon}$. It should also not be too large since we have neglected all other degrees of freedom, except for the two constituents, which would play a role at short distances. We thus vary the value of Λ_0 from 0.5 GeV to 1.2 GeV for an estimate of the two-body partial widths. In addition, an off-shell form factor for the exchanged meson with mass m , momentum q chosen as Eq. (14) needs to be introduced, and we take the form used in, e.g., Ref. [42].

$$f(q^2) = \frac{\Lambda_1^4}{(m^2 - q^2)^2 + \Lambda_1^4}, \quad (14)$$

The parameter Λ_1 for the off-shell form factor varies for different system, and we will vary it in the range of 1.5 \sim 2.4 GeV [43].

Taking all into account, we can easily get the partial widths of the $P_c(4380)$ decaying into all possible final states in both $\bar{D}\Sigma_c^*$ and $\bar{D}^*\Sigma_c$ molecular pictures. Partial decay widths of the $P_c(4450)$ state as a $\bar{D}^*\Sigma_c$ molecule with $J^P = 3/2^-$ can also be obtained. Except for the decay modes shown in Fig. 3, the $\bar{D}\Sigma_c^*$ mode is also allowed kinematically, and the diagram corresponding to this channel is shown in Fig. 4.

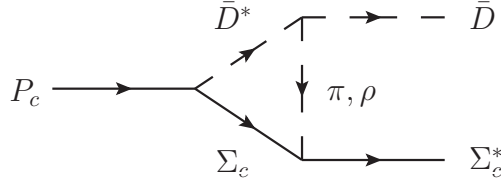


Figure 4: The $\bar{D}\Sigma_c^*$ decay channel of the $P_c(4450)$ state as a $\bar{D}^*\Sigma_c(2455)$ molecule.

3 Decay widths of the P_c states

Using the values of coupling constants listed in the Table 2, the partial decay widths of the P_c states are calculated in both $\bar{D}\Sigma_c^*$ and $\bar{D}^*\Sigma_c$ molecular pictures. Results obtained with typical cutoff values $\Lambda_0 = 1.0$ GeV and $\Lambda_1 = 2.0$ GeV are displayed in Table 3. However, these values should not be regarded as the final results of our calculation. Our model bears a large uncertainty due to the values of some of the coupling constants and the choice of cutoffs Λ_0 and Λ_1 . The dependence of the $P_c(4380)$ total width on the cutoff Λ_0 in different scenarios, together with the branching fractions of the three most relevant channels $\bar{D}^*\Lambda_c$, $\bar{D}\Lambda_c$ and $J/\psi p$, is shown in Fig. 5, and the dependence on Λ_1 is shown in Fig. 6. The ranges of the cutoff values are chosen as $\Lambda_0 \in [0.5, 1.2]$ GeV and $\Lambda_1 \in [1.5, 2.4]$ GeV. It should be mentioned that among the two-body decay modes of the $\bar{D}\Sigma_c^*$ molecule, the $\bar{D}^*\Lambda_c$, $J/\psi p$ and $\bar{D}\Lambda_c$ channels contribute most of widths. Therefore, we only focus on these channels for the cutoff dependence for simplicity.

The numerical results show that the $P_c(4380)$ state in both $\bar{D}\Sigma_c^*$ and $\bar{D}^*\Sigma_c$ molecular pictures has the $\bar{D}^*\Lambda_c$ as its largest decay channel. However, for the $\bar{D}\Lambda_c$ channel, the partial width in the $\bar{D}\Sigma_c^*$ picture for $P_c(4380)$ is much smaller than that in the $\bar{D}^*\Sigma_c$ picture. In addition, the relative ratio between branching fractions for the $\bar{D}^*\Lambda_c$ and $J/\psi p$ channels is very different in these two kinds of molecular scenarios. In the $J^P = \frac{3}{2}^-$ $\bar{D}\Sigma_c^*$ molecular picture, $\text{Br}(\bar{D}^*\Lambda_c) : \text{Br}(J/\psi p) \simeq 40 : 1$ when the cutoffs are fixed as $\Lambda_0 = 1.0$ GeV and $\Lambda_1 = 2$ GeV, while it is about 5 : 1 in

Table 3: Partial widths of $P_c(4380)$ as $\bar{D}\Sigma_c^*$ molecule and $\bar{D}^*\Sigma_c$ molecule respectively, and $P_c(4450)$ as $\bar{D}^*\Sigma_c$ molecule, to different possible final states with $\Lambda_0 = 1.0$ GeV, $\Lambda_1 = 2.0$ GeV. All of the decay widths are in the unit of MeV, and the short bars denote that the $\bar{D}\Sigma_c^*$ channel is closed in the $P_c(4380)$ molecule decay or the corresponding contribution is negligible.

Mode	Widths (MeV)			
	$P_c(4380)$		$P_c(4450)$	
	$\bar{D}\Sigma_c^*(\frac{3}{2}^-)$	$\bar{D}^*\Sigma_c(\frac{3}{2}^-)$	$\bar{D}^*\Sigma_c(\frac{3}{2}^-)$	$\bar{D}^*\Sigma_c(\frac{5}{2}^+)$
$\bar{D}^*\Lambda_c$	131.3	41.6	80.5	22.6
$J/\psi p$	3.8	8.4	8.3	2.0
$\bar{D}\Lambda_c$	1.2	17.0	41.4	18.8
πN	0.06	0.05	0.05	0.1
$\chi_{c0} p$	0.9	0.002	0.01	0.001
$\eta_c p$	0.2	0.08	0.1	0.04
ρN	1.4	0.08	0.07	0.1
ωp	5.3	0.3	0.3	0.2
$\bar{D}\Sigma_c$	0.01	0.1	1.2	0.8
$\bar{D}\Sigma_c^*$	-	-	7.7	1.4
$\bar{D}\Lambda_c\pi$	11.6	-	-	-
Total	144.3	67.7	139.7	46.2

the $J^P = \frac{3}{2}^- \bar{D}^*\Sigma_c$ picture with these cutoffs. In particular, as one can see from Figs. 5 and 6, this conspicuous difference holds for the whole ranges of cutoff values that we use for Λ_0 and Λ_1 . Hence, such an interesting feature should be rather model-independent, and should be extremely helpful for revealing the internal structure of the $P_c(4380)$ in future experiments. Furthermore, the decay width is more sensitive to the cut off Λ_0 in the regulators than Λ_1 in the off-shell form factor. This is determined by their specific forms.

It is clear that the total width of the $P_c(4380)$ in the $J^P = \frac{3}{2}^- \bar{D}\Sigma_c^*$ picture is larger than that in the $\bar{D}^*\Sigma_c$ picture. Thus, the former picture seems to be more consistent with the large measured width of around 200 MeV for the $P_c(4380)$ although the latter cannot be completely excluded given the large uncertainties of both experimental measurements and our theoretical estimates. In any case, the dominant decay mode of the $P_c(4380)$ is the $\bar{D}^*\Lambda_c$ which can proceed through one-pion exchange. Two previous calculations [7, 44] have underestimated the partial decay width of this channel. Ref. [7] only considered vector-meson exchanges and overlooked the

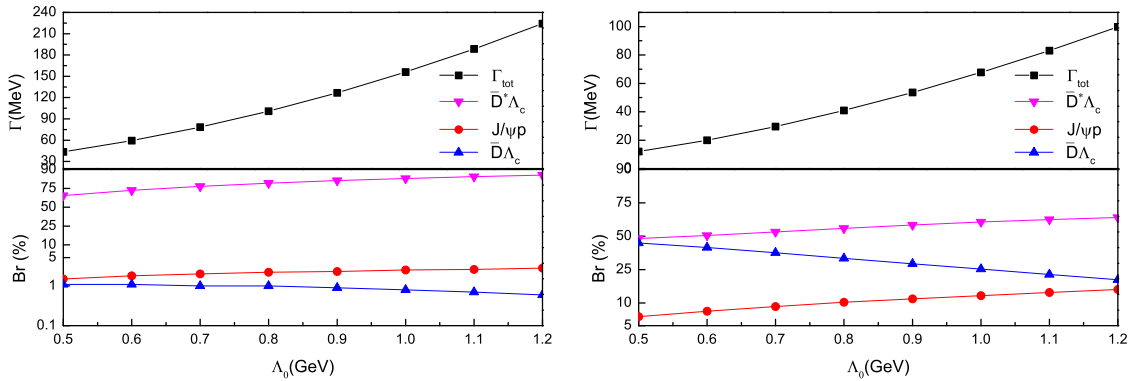


Figure 5: Dependence of the $P_c(4380)$ total width and branching fractions of $\bar{D}^*\Lambda_c$, $\bar{D}\Lambda_c$ and $J/\psi p$ on the cutoff Λ_0 in different scenarios for the $P_c(4380)$: (a) S -wave $\bar{D}\Sigma_c^*$ molecule with $J^P = \frac{3}{2}^-$; (b) S -wave $\bar{D}^*\Sigma_c$ molecule with $J^P = \frac{3}{2}^-$. Here Λ_1 is fixed at 2.0 GeV.

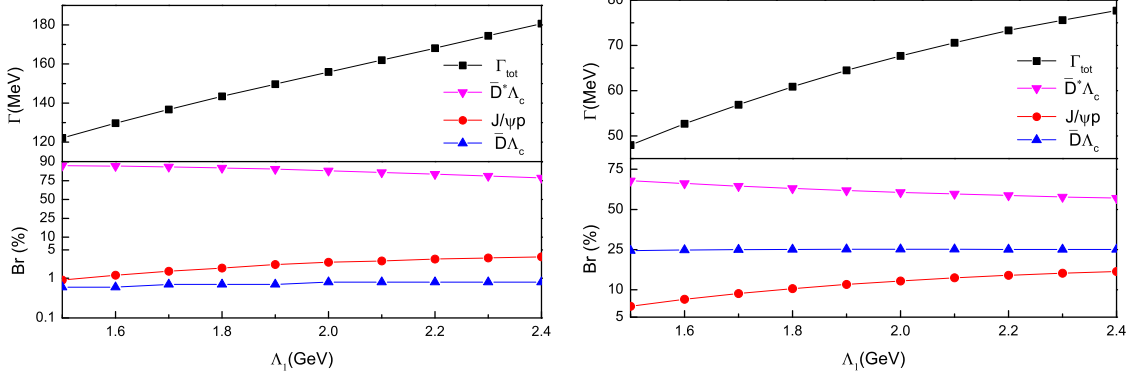


Figure 6: Dependence of the $P_c(4380)$ total width and branching fractions of $\bar{D}^*\Lambda_c$, $\bar{D}\Lambda_c$ and $J/\psi p$ on the cutoff Λ_1 in different scenarios for the $P_c(4380)$: (a) S -wave $\bar{D}\Sigma_c^*$ molecule with $J^P = \frac{3}{2}^-$; (b) S -wave $\bar{D}^*\Sigma_c$ molecule with $J^P = \frac{3}{2}^-$. Here Λ_0 is fixed at 1.0 GeV.

pion exchange contribution, while Ref. [44] calculated the meson-baryon interaction from the qq interaction in constituent quark model by using the resonating group method, which sometimes fails to reproduce hadronic observables. In fact, the pion exchange has also been found to be important for the $\bar{D}^*\Sigma_c - \bar{D}\Sigma_c^*$ coupled channel effects [45, 46].

The total decay width of the $P_c(4450)$ state described as a $J^P = \frac{3}{2}^-$ $\bar{D}^*\Sigma_c$ molecule is 140 MeV with $\Lambda_0 = 1.0$ GeV and $\Lambda_1 = 2.0$ GeV. This value is almost three times larger than the experimental one reported by the LHCb. One may reproduce the experimental value by taking the Λ_0 and Λ_1 values different from the ones used for the $P_c(4380)$ as an S -wave $\bar{D}\Sigma_c^*$ molecule. Another possibility is that the $P_c(4450)$ has quantum numbers $J^P = \frac{5}{2}^+$, hence could be a P -wave $\bar{D}^*\Sigma_c$ molecule. We will discuss this possibility in the following.

To estimate the partial widths of the $J^P = \frac{5}{2}^+$ $P_c(4450)$ state, we use the effective Lagrangian for the P -wave interaction among $P_c(4450)$, \bar{D}^* and Σ_c given by [28]

$$\mathcal{L}_{\bar{D}^*\Sigma_c P_c} = g_{\bar{D}^*\Sigma_c P_c} \left(-g^{\nu\alpha} + \frac{p^\nu p^\alpha}{p^2} \right) (\partial_\alpha \bar{\Sigma}_c \bar{D}^{*\mu} - \bar{\Sigma}_c \partial_\alpha \bar{D}^{*\mu}) P_{c\mu\nu} + H.c., \quad (15)$$

with p the momentum of the P_c state. In analogy with the S -wave interactions described by Eq. (1), the coupling constant $g_{\bar{D}^*\Sigma_c P_c}$ may be obtained from the compositeness condition [47, 48]. However, being in a P -wave, the obtained coupling strength relies much more on the cutoff Λ_0 . Thus, we can only make a rough estimate for the widths in this case. The corresponding numerical results obtained with $\Lambda_0 = 1.0$ GeV and $\Lambda_1 = 2.0$ GeV are listed in Table 3. The total width of the $\frac{5}{2}^+$ $\bar{D}^*\Sigma_c$ molecule is about 46 MeV with these cutoff values. The dependence on the cutoffs Λ_0 and Λ_1 in both $\frac{5}{2}^+$ and $\frac{3}{2}^-$ $\bar{D}^*\Sigma_c$ scenarios are presented in Figs. 7 and 8, respectively.

From the curves of branch ratios, we see that despite of the sizeable cutoff dependence of the total decay widths, the branching fractions are rather insensitive to the cutoff values. The decay behaviors in both the $\frac{5}{2}^+$ and $\frac{3}{2}^-$ $\bar{D}^*\Sigma_c$ molecular scenarios are similar to each other except for two points: the total decay width and the branch ratio of the $\bar{D}\Lambda_c$ channel. One sees that within the chosen cutoff ranges the total width of the $\frac{5}{2}^+$ $\bar{D}^*\Sigma_c$ molecule is almost always much smaller than that in the $\frac{3}{2}^-$ case, and the former is in much better agreement with the width reported by the LHCb Collaboration for the $P_c(4450)$, $(39 \pm 5 \pm 19)$ MeV. From this point of view, the $\bar{D}^*\Sigma_c$ molecule with $J^P = \frac{5}{2}^+$ seems to be a more favorable assignment for the $P_c(4450)$. The other difference is that the branching fraction of the $\bar{D}\Lambda_c$ channel is comparable with that of the $\bar{D}^*\Lambda_c$ channel in $J^P = \frac{5}{2}^+$ picture, while it is much smaller in the $J^P = \frac{3}{2}^-$ picture. Note that the partial width of the $\bar{D}\Lambda_c$ channel decreases with increasing Λ_0 , which leads to decreasing behavior of the total width of the $\frac{5}{2}^+$ $P_c(4450)$ for $\Lambda_0 \in [0.5, 0.9]$ GeV with $\Lambda_1 = 2.0$ GeV.

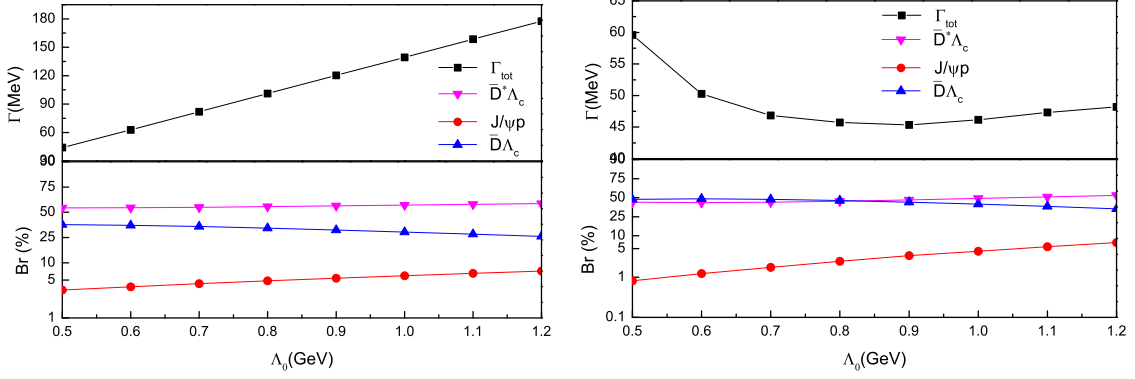


Figure 7: Dependence of the $P_c(4450)$ total width and branching fractions of $\bar{D}^*\Lambda_c$, $\bar{D}\Lambda_c$ and $J/\psi p$ on the cutoff Λ_0 in different scenarios for the $P_c(4380)$: (a) S -wave $\bar{D}^*\Sigma_c$ molecule with $J^P = \frac{3}{2}^-$; (b) P -wave $\bar{D}^*\Sigma_c$ molecule with $J^P = \frac{5}{2}^+$. Here Λ_1 is fixed at 2.0 GeV.

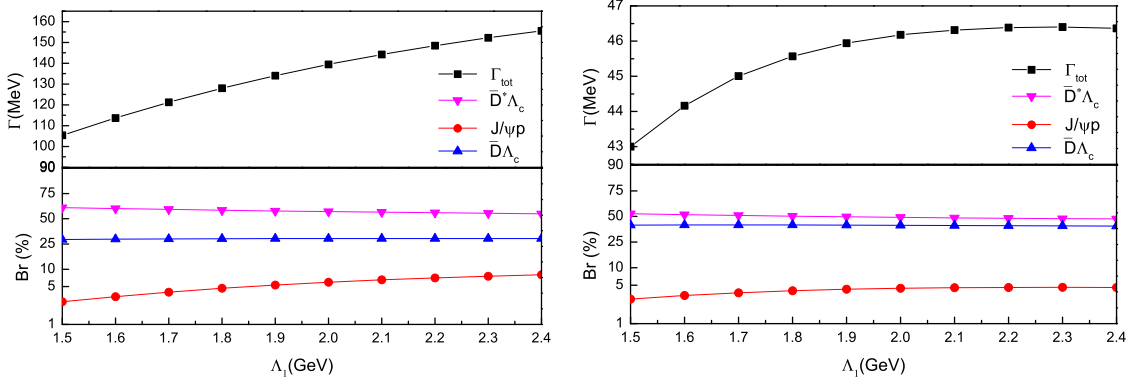


Figure 8: Dependence of the $P_c(4450)$ total width and branching fractions of $\bar{D}^*\Lambda_c$, $\bar{D}\Lambda_c$ and $J/\psi p$ on the cutoff Λ_1 in different scenarios for the $P_c(4380)$: (a) S -wave $\bar{D}^*\Sigma_c$ molecule with $J^P = \frac{3}{2}^-$; (b) P -wave $\bar{D}^*\Sigma_c$ molecule with $J^P = \frac{5}{2}^+$. Here Λ_0 is fixed at 1.0 GeV.

4 Production of P_c states in photo- and pion-induced reactions

In order to further pin down the nature of the P_c states, it would be very useful to study them through various two-body scattering processes [49–52]. In particular, this is extremely important so as to distinguish the resonance scenario from the kinematical singularities [24–27]. With the formalism given in the previous section, we can also estimate the total cross sections for some common scattering reactions with the $P_c(4380)$ as the intermediate state, for example the γp and πp collisions with the $J/\psi p$ as the final state, shown in Fig. 9. Note that the contribution from the u -channel exchange of the $P_c(4380)$ is negligible compared to the s -channel one since the intermediate P_c in u -channel processes will be highly off-shell. Therefore, only the s -channel contribution is included in our calculation. It is similar for the $P_c(4450)$ exchange.

We consider the possibility of $J^P = \frac{3}{2}^-$ for the $P_c(4380)$. The $p\pi P_c$ and $pJ/\psi P_c(p\gamma P_c)$ vertices should be dominated by D -wave and S -wave, respectively. The effective Lagrangians for these two kinds of vertices are given by [50]

$$\mathcal{L}_{PBP_c} = g_{PBP_c} \bar{P}_c^\mu \gamma_5 \gamma_\nu \partial^\nu \partial_\mu P B + \text{H.c.}, \quad (16)$$

$$\mathcal{L}_{VBP_c} = -ig_{VBP_c} \bar{P}_c^\mu \gamma^\nu B F_{\mu\nu} + \text{H.c.}, \quad (17)$$

where P and B are the fields for the pion and proton, respectively, $F_{\mu\nu} = \partial_\mu V_\nu - \partial_\nu V_\mu$ with V

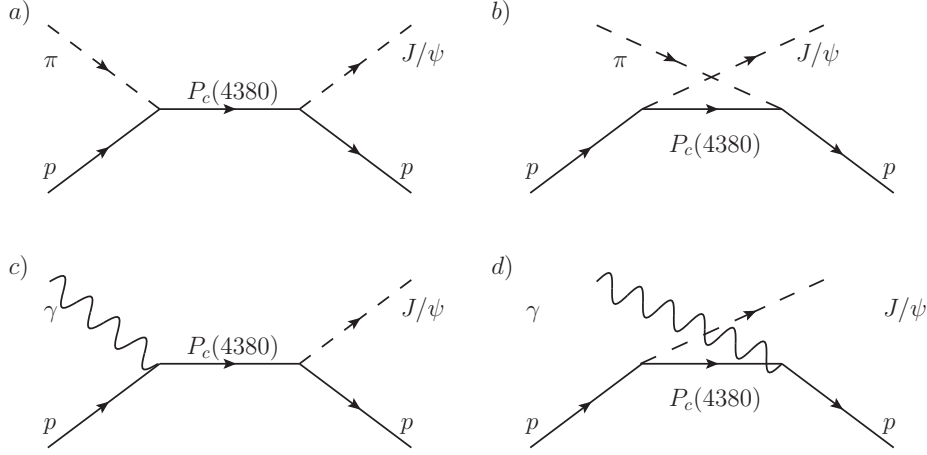


Figure 9: The s and u -channel reactions with the $P_c(4380)$ as the intermediate state, where $P_c(4380)$ is treated as the $\bar{D}\Sigma_c^*$ molecule with spin-parity $\frac{3}{2}^-$. a)&b) The s and u -channel contribution of the scattering process $p\pi \rightarrow J/\psi p$. c)&d) The s and u -channel contribution of the scattering process $p\gamma \rightarrow J/\psi p$.

the field for the photon or J/ψ .

To study these two reactions in Fig. 9, we need to get the related coupling constants $g_{pJ/\psi P_c}$, $g_{p\pi P_c}$ and $g_{p\gamma P_c}$. These coupling constants can be deduced from the partial widths of the P_c state decaying into $J/\psi p$, πp and $p\gamma$, respectively, which are estimated by calculating the triangle diagrams as in Section 3, where the partial widths for the $p\pi$ and pJ/ψ have been calculated. For the $p\gamma$ channel, the needed triangle diagram is shown in Fig. 10. The values of these couplings

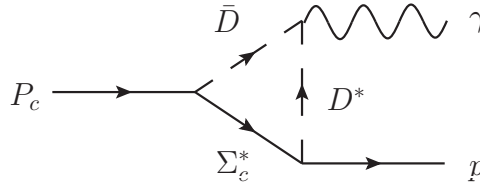


Figure 10: The decay of the P_c state into $p\gamma$.

and the partial widths of the $P_c(4380)$ as a $J^P = \frac{3}{2}^- \bar{D}\Sigma_c^*$ molecule that we will use in estimating the cross sections are listed in Table 4.

Table 4: Partial widths and couplings of $P_c(4380)$ as a $J^P = \frac{3}{2}^- \bar{D}\Sigma_c^*$ molecule into $J/\psi p$, πp and $p\gamma$ final states calculated with $\Lambda_0 = 1.0$ GeV, $\Lambda_1 = 2.0$ GeV.

Modes	Widths(MeV)	Couplings
$J/\psi p$	3.8	0.11 (GeV^{-1})
πp	0.06	0.0053 (GeV^{-2})
$p\gamma$	0.0007	0.00097 (GeV^{-1})

With the above Lagrangians and coupling constants, the cross sections can be estimated immediately by computing the tree diagrams shown in Fig. 10. The numerical results are given in Fig. 11. The clear peak structure in the cross sections is due to the s -channel exchange of the $P_c(4380)$ resonance in the reactions $p\pi \rightarrow J/\psi p$ and $p\gamma \rightarrow J/\psi p$.

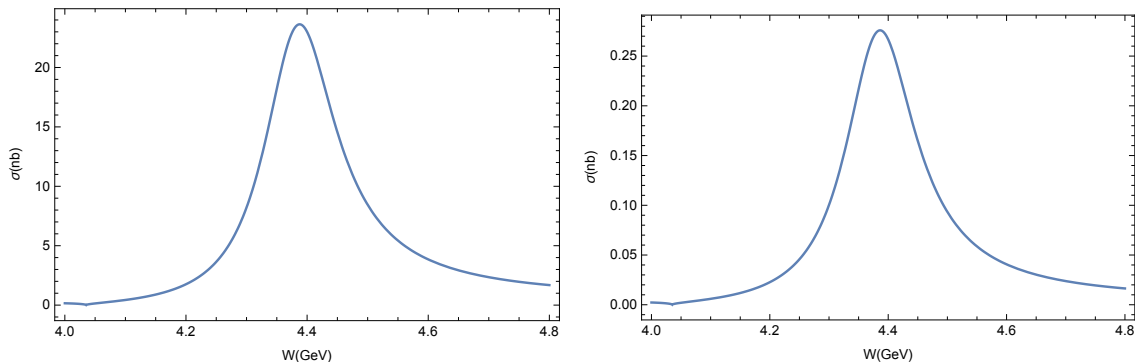


Figure 11: Dependence of the total cross sections on the center-of-mass energy W for the reactions (a) $p\pi \rightarrow J/\psi p$ and (b) $p\gamma \rightarrow J/\psi p$.

The numerical calculation suggests that the probability for the πp to $J/\psi p$ through $P_c(4380)$ molecule is two orders of magnitude larger than that in the γp collisions. This can be easily understood as the photo-production cross section is roughly suppressed by a factor of the fine structure constant $\alpha = 1/137$. The cross sections of the processes $\pi p \rightarrow J/\psi p$ and $\gamma p \rightarrow J/\psi p$ reactions have been calculated in Refs. [50, 51] and [49, 52], respectively, by assuming that $J/\psi p$ and πp channels account for some specific percentages of the $P_c(4380)$ total width. In Refs. [49, 52], the coupling constant $g_{p\gamma P_c}$ was estimated using the vector-meson-dominance model by assuming that the photon couples through intermediate vector mesons (J/ψ in Ref. [49] and ω , ρ and J/ψ in Ref. [52]). The coupling constant $g_{pJ/\psi P_c}$ used in Ref. [52] is deduced from the partial width of $P_c \rightarrow pJ/\psi$ predicted in Ref. [4] prior to the P_c discovery. The estimation in Ref. [52] for the total cross section of $\gamma p \rightarrow J/\psi p$ is in the order of magnitude of 0.1 to 1 nb, which is in line with the result in Ref. [49] with the $g_{pJ/\psi P_c}$ obtained by assuming a 5% branching fraction for the $P_c \rightarrow J/\psi p$. Refs. [50] and [51] obtained different cross sections for the $\pi p \rightarrow J/\psi p$ by using different decay branching ratios for the $J/\psi p$ and $p\pi$ channels. The former claims the cross section of $p\pi \rightarrow J/\psi p$ is of order 1 μb by assuming the branching ratios are 10% and 1% for the $J/\psi p$ and $p\pi$ channels, respectively, while the result is at the level of 1 nb by assuming branching fractions of 5% and 10^{-5} for the $J/\psi p$ and $p\pi$ channels, respectively, in Ref. [51]. However, in our work, we have obtained the partial widths of $P_c(4380)$ into these channels in the preceding calculations. Based on the results obtained using $\Lambda_0 = 1.0$ GeV, $\Lambda_1 = 2.0$ GeV, the total decay width of $P_c(4380)$ is 144 MeV, and the branching ratios of $J/\psi p$ and $p\pi$ channels are around 3% and 0.04%, respectively. Apparently, the cross sections of these tree diagrams are determined by these values. The parameters obtained from our calculations are different from the assumptions in these literature, and thus we obtain different cross sections.

In addition, another interesting conclusion can be deduced from our numerical results. As shown in Table 3, the $\bar{D}^*\Lambda_c$ and $\bar{D}\Lambda_c$ channels should be the dominant channels for both the $P_c(4380)$ as a $J^P = \frac{3}{2}^- \bar{D}\Sigma_c^*$ molecule and the $P_c(4450)$ as a $J^P = \frac{5}{2}^+ \bar{D}^*\Sigma_c$ molecule. Their partial widths are much larger than that of the $J/\psi p$. This means that the cross sections of the processes $\pi p \rightarrow \bar{D}^*\Lambda_c$ and $\pi p \rightarrow \bar{D}\Lambda_c$ through $P_c(4380)$ and $P_c(4450)$ must be much larger than the reaction $\pi p \rightarrow J/\psi p$. It is consistent with the claims in Refs. [51, 53]. In conclusion, from the point of view of cross sections, it should be easier to search for the pentaquark states with hidden-charm in the $\bar{D}^*\Lambda_c$ and $\bar{D}\Lambda_c$ production than the $J/\psi p$ production.

5 Summary

An interesting property of the two P_c structures reported by the LHCb Collaboration in 2015 is that they are located just below the $\bar{D}\Sigma_c^*(2520)$ and $\bar{D}^*\Sigma_c(2455)$ thresholds, respectively. Inspired by this property, the two P_c states were proposed to be either $\bar{D}\Sigma_c^*$ or $\bar{D}^*\Sigma_c$ S -wave bound states of spin-parity $J^P = \frac{3}{2}^-$. We estimated the decay behaviors of such two types of hadronic molecules

in this paper. With branching ratios of ten possible decay channels calculated, it is found that the two types of hadronic molecules have distinguishable decay patterns. While the $\bar{D}\Sigma_c^*$ molecule decays dominantly to the $\bar{D}^*\Lambda_c$ channel with a branching ratio by two orders of magnitude larger than that to the $\bar{D}\Lambda_c$, the $\bar{D}^*\Sigma_c$ molecule decays into these two channels with a difference of less than a factor of 2. Our results show that the total decay width of $P_c(4380)$ as a $\frac{3}{2}^- \bar{D}\Sigma_c^*$ molecule is about a factor of 2 larger than the corresponding value for the $\bar{D}^*\Sigma_c$ molecule. It seems to suggest that the assignment of $\bar{D}\Sigma_c^*$ molecule for the $P_c(4380)$ is more favorable than the $\bar{D}^*\Sigma_c$ molecule. The results for the $P_c(4450)$ indicate that the $P_c(4450)$ is more likely a $J^P = \frac{5}{2}^+ \bar{D}^*\Sigma_c$ P -wave molecule than an $\frac{3}{2}^- \bar{D}^*\Sigma_c$ S -wave molecule. In order to further pin down the nature of the P_c states, it would be very useful to study them through various two-body scattering processes. Based on the partial decay widths of the $P_c(4380)$, we estimated the cross sections for the reactions $\gamma p \rightarrow J/\psi p$ and $\pi p \rightarrow J/\psi p$ through exchanging the $P_c(4380)$ state in the s -channel. The peak values are at the level of 0.2 nb and 20 nb, respectively. The corresponding productions rates for reactions into $\bar{D}^*\Lambda_c$ and/or $\bar{D}\Lambda_c$ would be larger by orders of magnitude. The forthcoming γp experiment at JLAB and πp experiment at JPARC should be able to provide valuable information towards revealing the nature of these P_c structures.

Acknowledgments

We thank Yu Lu for helps on computing program. This project is supported by NSFC under Grant No. 11261130311 (CRC110 cofunded by DFG and NSFC) and Grant No. 11647601, and by the Thousand Talents Plan for Young Professionals, and by the CAS Key Research Program of Frontier Sciences under Grant No. QYZDB-SSW-SYS013.

Appendix: decay amplitudes

This appendix collects together all the formulae that are used in the calculations of the scattering amplitudes in our work. Except for the $\chi_{c0}p$ final states described by diagram $e)$, $e')$ in Fig. 2, 3, and the $\bar{D}\Sigma_c^*$ channels shown in Fig. 4, the other two-body decays for the two P_c states can be classified into the categories shown in Fig. 12.

The corresponding amplitudes can be written as

$$\begin{aligned}
\mathcal{M}_1 = & g_{\bar{D}\Sigma_c^*P_c} g_{VP_1P_2} g_{VBB_1^*} \int_{-\infty}^{\infty} \frac{d^4k}{(2\pi)^4} \left\{ \tilde{\Phi} \left[\frac{m_{\bar{D}}}{m_{\bar{D}} + m_{\Sigma_c^*}} p_0 - (p_1 + k) \right] \frac{\Lambda_1^4}{(m_V^2 - k^2)^2 + \Lambda_1^4} \right. \\
& \bar{u}(p_1, s_B) \gamma^\alpha \gamma_5 \frac{1}{k^2 - m_V^2} \left[k_\mu \left(g_{\alpha\beta} - \frac{k_\alpha k_\beta}{m_V^2} \right) - k_\alpha \left(g_{\mu\beta} - \frac{k_\mu k_\beta}{m_V^2} \right) \right] \\
& \frac{\not{p}_1 + \not{k} + m_{\Sigma_c^*}}{(p_1 + k)^2 - m_{\Sigma_c^*}^2 + im_{\Sigma_c^*} \Gamma_{\Sigma_c^*}} \left[-g^{\mu\nu} + \frac{1}{3} \gamma^\mu \gamma^\nu + \frac{1}{3m_{\Sigma_c^*}} (\gamma^\mu (p_1 + k)^\nu - \gamma^\nu (p_1 + k)^\mu) + \right. \\
& \left. \left. \frac{2}{3m_{\Sigma_c^*}^2} (p_1 + k)^\mu (p_1 + k)^\nu \right] [-2(p_0 - p_1) + k]^\beta \frac{1}{(p_0 - p_1 - k)^2 - m_{P_1}^2} u_\nu(p_0, s_{P_c}) \right\}, \quad (18)
\end{aligned}$$

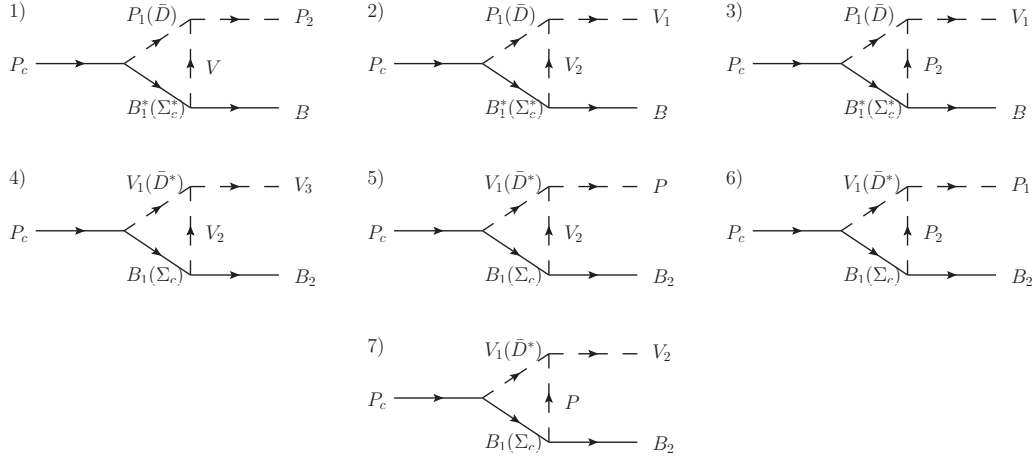


Figure 12: Various kinds of triangle diagrams for the two-body decays of the P_c state. 1) The $\bar{D}\Lambda_c$ channel with ρ exchange, πN channel with D^* exchange, $\eta_c p$ channel with D^* exchange and $\bar{D}\Sigma_c$ channel with ρ exchange for the $\bar{D}\Sigma_c^*$ hadronic molecule of $P_c(4380)$. 2) $\bar{D}^*\Lambda_c$ channel with ρ exchange, $J/\psi p$ channel with D^* exchange, ρN channel with D^* exchange and ωp channel with D^* exchange for the $\bar{D}\Sigma_c^*$ hadronic molecule of $P_c(4380)$. 3) $\bar{D}^*\Lambda_c$ channel with π exchange, $J/\psi p$ channel with D exchange and ωp channel with D exchange for the $\bar{D}\Sigma_c^*$ hadronic molecule of $P_c(4380)$. 4) $\bar{D}^*\Lambda_c$ channel with ρ exchange, $J/\psi p$ channel with D^* exchange, ρN channel with D^* exchange and ωp channel with D^* exchange for the $\bar{D}^*\Sigma_c$ hadronic molecules of $P_c(4380)$ and $P_c(4450)$. 5) The $\bar{D}\Lambda_c$ channel with ρ exchange, πN channel with D^* exchange, $\eta_c p$ channel with D^* exchange and $\bar{D}\Sigma_c$ channel with ρ exchange for the $\bar{D}^*\Sigma_c$ hadronic molecules of $P_c(4380)$ and $P_c(4450)$. 6) The $\bar{D}\Lambda_c$ channel with π exchange, πN channel with D exchange, $\eta_c p$ channel with D exchange and $\bar{D}\Sigma_c$ channel with π exchange for the $\bar{D}^*\Sigma_c$ hadronic molecules of $P_c(4380)$ and $P_c(4450)$. 7) $\bar{D}^*\Lambda_c$ channel with π exchange, $J/\psi p$ channel with D exchange, ρN channel with D exchange and ωp channel with D exchange for the $\bar{D}^*\Sigma_c$ hadronic molecules of $P_c(4380)$ and $P_c(4450)$.

$$\begin{aligned}
\mathcal{M}_2 = & g_{\bar{D}\Sigma_c^* P_c} g_{V_1 V_2 P_1} g_{V_2 B B_1^*} \int_{-\infty}^{\infty} \frac{d^4 k}{(2\pi)^4} \left\{ \tilde{\Phi} \left[\frac{m_{\bar{D}}}{m_{\bar{D}} + m_{\Sigma_c^*}} p_0 - (p_1 + k) \right] \frac{\Lambda_1^4}{(m_{V_2}^2 - k^2)^2 + \Lambda_1^4} \right. \\
& \bar{u}(p_1, s_B) \gamma^\alpha \gamma_5 \frac{1}{k^2 - m_{V_2}^2} \left[k_\mu \left(g_{\alpha\beta} - \frac{k_\alpha k_\beta}{m_{V_2}^2} \right) - k_\alpha \left(g_{\mu\beta} - \frac{k_\mu k_\beta}{m_{V_2}^2} \right) \right] \\
& \frac{p_1 + k + m_{\Sigma_c^*}}{(p_1 + k)^2 - m_{\Sigma_c^*}^2 + i m_{\Sigma_c^*} \Gamma_{\Sigma_c^*}} \left[-g^{\mu\nu} + \frac{1}{3} \gamma^\mu \gamma^\nu + \frac{1}{3 m_{\Sigma_c^*}} (\gamma^\mu (p_1 + k)^\nu - \gamma^\nu (p_1 + k)^\mu) + \right. \\
& \left. \frac{2}{3 m_{\Sigma_c^*}^2} (p_1 + k)^\mu (p_1 + k)^\nu \right] \varepsilon^{\rho\sigma\lambda\beta} [-(p_0 - p_1)_\rho \epsilon_\sigma^* (p_0 - p_1, s_{V_1}) k_\lambda] \frac{1}{(p_0 - p_1 - k)^2 - m_{P_1}^2} \\
& \left. u_\nu(p_0, s_{P_c}) \right\}, \tag{19}
\end{aligned}$$

$$\begin{aligned}
\mathcal{M}_3 = & -g_{\bar{D}\Sigma_c^* P_c} g_{V_1 P_1 P_2} g_{P_2 B B_1^*} \int_{-\infty}^{\infty} \frac{d^4 k}{(2\pi)^4} \left\{ \tilde{\Phi} \left[\frac{m_{\bar{D}}}{m_{\bar{D}} + m_{\Sigma_c^*}} p_0 - (p_1 + k) \right] \frac{\Lambda_1^4}{(m_{P_2}^2 - k^2)^2 + \Lambda_1^4} \right. \\
& \bar{u}(p_1, s_B) k_\mu \frac{p_1 + k + m_{\Sigma_c^*}}{(p_1 + k)^2 - m_{\Sigma_c^*}^2 + i m_{\Sigma_c^*} \Gamma_{\Sigma_c^*}} \left[-g^{\mu\nu} + \frac{1}{3} \gamma^\mu \gamma^\nu + \frac{1}{3 m_{\Sigma_c^*}} (\gamma^\mu (p_1 + k)^\nu - \right. \\
& \left. \gamma^\nu (p_1 + k)^\mu) + \frac{2}{3 m_{\Sigma_c^*}^2} (p_1 + k)^\mu (p_1 + k)^\nu \right] [2k - (p_0 - p_1)]^\beta \epsilon_\beta^* (p_0 - p_1, s_{V_1}) \\
& \left. \frac{1}{k^2 - m_{P_2}^2} \frac{1}{(p_0 - p_1 - k)^2 - m_{P_1}^2} u_\nu(p_0, s_{P_c}) \right\}, \tag{20}
\end{aligned}$$

$$\begin{aligned}
\mathcal{M}_4 = & -ig_{\bar{D}^*\Sigma_c P_c} g_{V_1 V_2 V_3} g_{V_2 B_1 B_2} \int_{-\infty}^{\infty} \frac{d^4 k}{(2\pi)^4} \left\{ \tilde{\Phi} \left[\frac{m_{\bar{D}^*}}{m_{\bar{D}^*} + m_{\Sigma_c}} p_0 - (p_1 + k) \right] \frac{\Lambda_1^4}{(m_{V_2}^2 - k^2)^2 + \Lambda_1^4} \right. \\
& \bar{u}(p_1, s_{B_2}) \gamma^\alpha \frac{1}{k^2 - m_{V_2}^2} \left(g_{\alpha\beta} - \frac{k_\alpha k_\beta}{m_{V_2}^2} \right) \frac{p_1 + k + m_{\Sigma_c}}{(p_1 + k)^2 - m_{\Sigma_c}^2} \left[(2k - (p_0 - p_1))^\mu g^{\beta\sigma} + \right. \\
& \left. \left. (-p_0 - p_1 - k)^\sigma g^{\mu\beta} + (2(p_0 - p_1) - k)^\beta g^{\mu\sigma} \right] \frac{1}{(p_0 - p_1 - k)^2 - m_{V_1}^2} \right. \\
& \left. \left(g_{\sigma\nu} - \frac{(p_0 - p_1 - k)_\sigma (p_0 - p_1 - k)_\nu}{m_{V_1}^2} \right) \epsilon_\mu^*(p_0 - p_1, s_{V_3}) u^\nu(p_0, s_{P_c}) \right\}, \quad (21)
\end{aligned}$$

$$\begin{aligned}
\mathcal{M}_5 = & ig_{\bar{D}^*\Sigma_c P_c} g_{V_1 V_2 P} g_{V_2 B_1 B_2} \int_{-\infty}^{\infty} \frac{d^4 k}{(2\pi)^4} \left\{ \tilde{\Phi} \left[\frac{m_{\bar{D}^*}}{m_{\bar{D}^*} + m_{\Sigma_c}} p_0 - (p_1 + k) \right] \frac{\Lambda_1^4}{(m_{V_2}^2 - k^2)^2 + \Lambda_1^4} \right. \\
& \bar{u}(p_1, s_{B_2}) \gamma^\mu \frac{p_1 + k + m_{\Sigma_c}}{(p_1 + k)^2 - m_{\Sigma_c}^2} \frac{1}{k^2 - m_{V_2}^2} \left(g_{\mu\alpha} - \frac{k_\mu k_\alpha}{m_{V_2}^2} \right) \varepsilon^{\rho\alpha\sigma\beta} [k_\rho (p_0 - p_1 - k)_\sigma] \\
& \left. \frac{1}{(p_0 - p_1 - k)^2 - m_{V_1}^2} \left[g^{\beta\nu} - \frac{(p_0 - p_1 - k)_\beta (p_0 - p_1 - k)_\nu}{m_{V_1}^2} \right] u^\nu(p_0, s_{P_c}) \right\}, \quad (22)
\end{aligned}$$

$$\begin{aligned}
\mathcal{M}_6 = & ig_{\bar{D}^*\Sigma_c P_c} g_{V_1 P_1 P_2} g_{P_2 B_1 B_2} \int_{-\infty}^{\infty} \frac{d^4 k}{(2\pi)^4} \left\{ \tilde{\Phi} \left[\frac{m_{\bar{D}^*}}{m_{\bar{D}^*} + m_{\Sigma_c}} p_0 - (p_1 + k) \right] \frac{\Lambda_1^4}{(m_{P_2}^2 - k^2)^2 + \Lambda_1^4} \right. \\
& \bar{u}(p_1, s_{B_2}) \gamma^5 \frac{p_1 + k + m_{\Sigma_c}}{(p_1 + k)^2 - m_{\Sigma_c}^2} \frac{1}{(p_0 - p_1 - k)^2 - m_{V_1}^2} \left[g^{\beta\nu} - \frac{(p_0 - p_1 - k)^\beta (p_0 - p_1 - k)^\nu}{m_{V_1}^2} \right] \\
& \left. (-p_0 - p_1 - k)_\beta \frac{1}{k^2 - m_P^2} u_\nu(p_0, s_{P_c}) \right\}, \quad (23)
\end{aligned}$$

$$\begin{aligned}
\mathcal{M}_7 = & ig_{\bar{D}^*\Sigma_c P_c} g_{V_1 V_2 P} g_{P B_1 B_2} \int_{-\infty}^{\infty} \frac{d^4 k}{(2\pi)^4} \left\{ \tilde{\Phi} \left[\frac{m_{\bar{D}^*}}{m_{\bar{D}^*} + m_{\Sigma_c}} p_0 - (p_1 + k) \right] \frac{\Lambda_1^4}{(m_P^2 - k^2)^2 + \Lambda_1^4} \right. \\
& \bar{u}(p_1, s_{B_2}) \gamma^5 \frac{p_1 + k + m_{\Sigma_c}}{(p_1 + k)^2 - m_{\Sigma_c}^2} \varepsilon^{\alpha\beta\lambda\rho} [(p_0 - p_1 - k)_\alpha (-p_0 - p_1)_\lambda \epsilon_\rho^*(p_0 - p_1, s_{V_2})] \\
& \frac{1}{(p_0 - p_1 - k)^2 - m_{V_1}^2} \left[g^{\beta\nu} - \frac{(p_0 - p_1 - k)_\beta (p_0 - p_1 - k)_\nu}{m_{V_1}^2} \right] \\
& \left. \frac{1}{k^2 - m_P^2} u^\nu(p_0, s_{P_c}) \right\}, \quad (24)
\end{aligned}$$

As for the $\chi_{c0} p$ and $\bar{D}\Sigma_c^*$ channels, the expressions of the amplitudes are given as,

$$\begin{aligned}
\mathcal{M}_{\chi_{c0} p - D} = & -ig_{\bar{D}\Sigma_c^* P_c} g_{\bar{D} D \chi_{c0}} g_{D P \Sigma_c^*} \int_{-\infty}^{\infty} \frac{d^4 k}{(2\pi)^4} \left\{ \tilde{\Phi} \left[\frac{m_{\bar{D}}}{m_{\bar{D}} + m_{\Sigma_c^*}} p_0 - (p_1 + k) \right] \frac{\Lambda_1^4}{(m_{\bar{D}}^2 - k^2)^2 + \Lambda_1^4} \right. \\
& \bar{u}(p_1, s_p) k_\mu \frac{p_1 + k + m_{\Sigma_c^*}}{(p_1 + k)^2 - m_{\Sigma_c^*}^2 + im_{\Sigma_c^*} \Gamma_{\Sigma_c^*}} \left[-g^{\mu\nu} + \frac{1}{3} \gamma^\mu \gamma^\nu + \frac{1}{3m_{\Sigma_c^*}} (\gamma^\mu (p_1 + k)^\nu - \right. \\
& \left. \left. \gamma^\nu (p_1 + k)^\mu) \frac{2}{3m_{\Sigma_c^*}^2} (p_1 + k)^\mu (p_1 + k)^\nu \right] \frac{1}{k^2 - m_D^2} \frac{1}{(p_0 - p_1 - k)^2 - m_D^2} \right. \\
& \left. u_\nu(p_0, s_{P_c}) \right\}, \quad (25)
\end{aligned}$$

$$\begin{aligned}
\mathcal{M}_{\chi_{c0}P-D^*} &= -g_{\bar{D}^*\Sigma_c P_c} g_{\bar{D}^* D^* \chi_{c0}} g_{D^* P \Sigma_c} \int_{-\infty}^{\infty} \frac{d^4 k}{(2\pi)^4} \left\{ \tilde{\Phi} \left[\frac{m_{\bar{D}^*}}{m_{\bar{D}^*} + m_{\Sigma_c}} p_0 - (p_1 + k) \right] \frac{\Lambda_1^4}{(m_{\bar{D}^*}^2 - k^2)^2 + \Lambda_1^4} \right. \\
&\quad \bar{u}(p_1, s_p) \gamma^\alpha \frac{1}{k^2 - m_{\bar{D}^*}^2} \left(g_{\alpha\beta} - \frac{k_\alpha k_\beta}{m_{\bar{D}^*}^2} \right) \frac{p_1 + k + m_{\Sigma_c}}{(p_1 + k)^2 - m_{\Sigma_c}^2} \frac{1}{(p_0 - p_1 - k)^2 - m_{\bar{D}^*}^2} \\
&\quad \left. \left[g^{\beta\nu} - \frac{(p_0 - p_1 - k)^\beta (p_0 - p_1 - k)^\nu}{m_{\bar{D}^*}^2} \right] u_\nu(p_0, s_{P_c}) \right\}, \tag{26}
\end{aligned}$$

$$\begin{aligned}
\mathcal{M}_{\bar{D}\Sigma_c^*-\pi} &= ig_{\bar{D}^*\Sigma_c P_c} g_{D^* D \pi} g_{\pi \Sigma_c \Sigma_c^*} \int_{-\infty}^{\infty} \frac{d^4 k}{(2\pi)^4} \left\{ \tilde{\Phi} \left[\frac{m_{\bar{D}^*}}{m_{\bar{D}^*} + m_{\Sigma_c}} p_0 - (p_1 + k) \right] \frac{\Lambda_1^4}{(m_\pi^2 - k^2)^2 + \Lambda_1^4} \right. \\
&\quad \bar{u}_\mu(p_1, s_{\Sigma_c^*}) k^\mu \frac{p_1 + k + m_{\Sigma_c}}{(p_1 + k)^2 - m_{\Sigma_c}^2} \frac{1}{(p_0 - p_1 - k)^2 - m_{\bar{D}^*}^2} \\
&\quad \left. \left[g^{\beta\nu} - \frac{(p_0 - p_1 - k)^\beta (p_0 - p_1 - k)^\nu}{m_{\bar{D}^*}^2} \right] \frac{-(p_0 - p_1)_\beta - k_\beta}{k^2 - m_\pi^2} u_\nu(p_0, s_{P_c}) \right\}, \tag{27}
\end{aligned}$$

$$\begin{aligned}
\mathcal{M}_{\bar{D}\Sigma_c^*-\rho} &= -ig_{\bar{D}^*\Sigma_c P_c} g_{D^* D \rho} g_{\rho \Sigma_c \Sigma_c^*} \int_{-\infty}^{\infty} \frac{d^4 k}{(2\pi)^4} \left\{ \tilde{\Phi} \left[\frac{m_{\bar{D}^*}}{m_{\bar{D}^*} + m_{\Sigma_c}} p_0 - (p_1 + k) \right] \frac{\Lambda_1^4}{(m_\rho^2 - k^2)^2 + \Lambda_1^4} \right. \\
&\quad \bar{u}^\mu(p_1, s_{\Sigma_c^*}) \gamma^\alpha \gamma_5 \frac{1}{k^2 - m_\rho^2} \left[k_\mu \left(g_{\alpha\beta} - \frac{k_\alpha k_\beta}{m_\rho^2} \right) - k_\alpha \left(g_{\mu\beta} - \frac{k_\mu k_\beta}{m_\rho^2} \right) \right] \\
&\quad \frac{p_1 + k + m_{\Sigma_c}}{(p_1 + k)^2 - m_{\Sigma_c}^2} \varepsilon^{\rho\sigma\lambda\beta} [(p_0 - p_1 - k)_\rho k_\lambda] \frac{1}{(p_0 - p_1 - k)^2 - m_{\bar{D}^*}^2} \\
&\quad \left. \left[g_{\sigma\nu} - \frac{(p_0 - p_1 - k)_\sigma (p_0 - p_1 - k)_\nu}{m_{\bar{D}^*}^2} \right] \frac{-(p_0 - p_1)_\beta - k_\beta}{k^2 - m_\pi^2} u^\nu(p_0, s_{P_c}) \right\}, \tag{28}
\end{aligned}$$

References

- [1] C. Patrignani *et al.* [Particle Data Group], *Chin. Phys. C* **40**, 100001 (2016).
- [2] H. X. Chen, W. Chen, X. Liu and S. L. Zhu, *Phys. Rept.* **639**, 1 (2016) [arXiv:1601.02092 [hep-ph]].
- [3] R. Aaij *et al.* [LHCb Collaboration], *Phys. Rev. Lett.* **115**, 072001 (2015) [arXiv:1507.03414 [hep-ex]].
- [4] J. J. Wu, R. Molina, E. Oset and B. S. Zou, *Phys. Rev. Lett.* **105** (2010) 232001 [arXiv:1007.0573 [nucl-th]]; *Phys. Rev. C* **84** (2011) 015202 [arXiv:1011.2399 [nucl-th]].
- [5] Z. C. Yang, Z. F. Sun, J. He, X. Liu and S. L. Zhu, *Chin. Phys. C* **36** (2012) 6 [arXiv:1105.2901 [hep-ph]].
- [6] S. G. Yuan, K. W. Wei, J. He, H. S. Xu and B. S. Zou, *Eur. Phys. J. A* **48** (2012) 61 [arXiv:1201.0807 [nucl-th]].
- [7] C. W. Xiao, J. Nieves and E. Oset, *Phys. Rev. D* **88** (2013) 056012 [arXiv:1304.5368 [hep-ph]].
- [8] Q. F. Lü and Y. B. Dong, arXiv:1603.00559 [hep-ph].

- [9] C. W. Shen, F. K. Guo, J. J. Xie and B. S. Zou, Nucl. Phys. A **954**, 393 (2016) [arXiv:1603.04672 [hep-ph]].
- [10] H. X. Chen, W. Chen, X. Liu, T. G. Steele and S. L. Zhu, Phys. Rev. Lett. **115**, 172001 (2015) [arXiv:1507.03717 [hep-ph]].
- [11] J. He, Phys. Lett. B **753**, 547 (2016) [arXiv:1507.05200 [hep-ph]].
- [12] L. Roca, J. Nieves and E. Oset, Phys. Rev. D **92**, 094003 (2015) [arXiv:1507.04249 [hep-ph]].
- [13] R. Chen, X. Liu, X. Q. Li and S. L. Zhu, Phys. Rev. Lett. **115**, 132002 (2015) [arXiv:1507.03704 [hep-ph]].
- [14] U.-G. Meißner and J. A. Oller, Phys. Lett. B **751**, 59 (2015) [arXiv:1507.07478 [hep-ph]].
- [15] C. W. Xiao and U.-G. Meißner, Phys. Rev. D **92**, 114002 (2015) [arXiv:1508.00924 [hep-ph]].
- [16] A. Ali, I. Ahmed, M. J. Aslam and A. Rehman, Phys. Rev. D **94**, 054001 (2016) [arXiv:1607.00987 [hep-ph]].
- [17] L. Maiani, A. D. Polosa and V. Riquer, Phys. Lett. B **749**, 289 (2015) [arXiv:1507.04980 [hep-ph]].
- [18] G. N. Li, X. G. He and M. He, JHEP **1512**, 128 (2015) [arXiv:1507.08252 [hep-ph]].
- [19] A. Mironov and A. Morozov, JETP Lett. **102**, 271 (2015) [Pisma Zh. Eksp. Teor. Fiz. **102**, 302 (2015)] [arXiv:1507.04694 [hep-ph]].
- [20] V. V. Anisovich, M. A. Matveev, J. Nyiri, A. V. Sarantsev and A. N. Semenova, arXiv:1507.07652 [hep-ph].
- [21] R. Ghosh, A. Bhattacharya and B. Chakrabarti, arXiv:1508.00356 [hep-ph].
- [22] Z. G. Wang, Eur. Phys. J. C **76**, 70 (2016) [arXiv:1508.01468 [hep-ph]].
- [23] V. Kubarovsky and M. B. Voloshin, Phys. Rev. D **92**, 031502 (2015) [arXiv:1508.00888 [hep-ph]].
- [24] F.-K. Guo, U.-G. Meißner, W. Wang and Z. Yang, Phys. Rev. D **92**, 071502 (2015) [arXiv:1507.04950 [hep-ph]].
- [25] X. H. Liu, Q. Wang and Q. Zhao, Phys. Lett. B **757**, 231 (2016) [arXiv:1507.05359 [hep-ph]].
- [26] F. K. Guo, U.-G. Meißner, J. Nieves and Z. Yang, Eur. Phys. J. A **52**, 318 (2016) [arXiv:1605.05113 [hep-ph]].
- [27] M. Bayar, F. Aceti, F.-K. Guo and E. Oset, Phys. Rev. D **94**, 074039 (2016) [arXiv:1609.04133 [hep-ph]].
- [28] B. S. Zou and F. Hussain, Phys. Rev. C **67** (2003) 015204 [hep-ph/0210164].
- [29] S. Weinberg, Phys. Rev. **137**, B672 (1965).
- [30] V. Baru, J. Haidenbauer, C. Hanhart, Y. Kalashnikova and A. E. Kudryavtsev, Phys. Lett. B **586**, 53 (2004) [hep-ph/0308129].
- [31] G. Erkol, R. G. E. Timmermans and T. A. Rijken, Phys. Rev. C **74**, 045201 (2006).
- [32] E. J. Garzon and J. J. Xie, Phys. Rev. C **92**, 035201 (2015). [arXiv:1506.06834 [hep-ph]].
- [33] Y. S. Oh, T. Song and S. H. Lee, Phys. Rev. C **63**, 034901 (2001) [nucl-th/0010064].

- [34] F.-K. Guo, C. Hanhart, G. Li, U.-G. Meißner and Q. Zhao, Phys. Rev. D **83**, 034013 (2011) [arXiv:1008.3632 [hep-ph]].
- [35] P. Colangelo, F. De Fazio and T. N. Pham, Phys. Rev. D **69**, 054023 (2004) [hep-ph/0310084].
- [36] Z. W. Lin and C. M. Ko, Phys. Rev. C **62**, 034903 (2000) [nucl-th/9912046].
- [37] D. Ronchen *et al.*, Eur. Phys. J. A **49**, 44 (2013) [arXiv:1211.6998 [nucl-th]].
- [38] T. M. Aliev, K. Azizi, M. Savci and V. S. Zamiralov, Phys. Rev. D **83**, 096007 (2011) [arXiv:1102.0416 [hep-ph]].
- [39] M. Albaladejo, F.-K. Guo, C. Hidalgo-Duque, J. Nieves and M. P. Valderrama, Eur. Phys. J. C **75**, 547 (2015) [arXiv:1504.00861 [hep-ph]].
- [40] Y. B. Dong, A. Faessler, T. Gutsche and V. E. Lyubovitskij, Phys. Rev. D **77**, 094013 (2008) [arXiv:0802.3610 [hep-ph]].
- [41] Y. Dong, A. Faessler, T. Gutsche, S. Kovalenko and V. E. Lyubovitskij, Phys. Rev. D **79**, 094013 (2009) [arXiv:0903.5416 [hep-ph]].
- [42] J. He, Phys. Rev. C **91**, 018201 (2015) [arXiv:1501.00522 [nucl-th]].
- [43] J. He and P. L. Lü, Chin. Phys. C **40**, 043101 (2016) [arXiv:1410.8645 [hep-ph]].
- [44] P. G. Ortega, D. R. Entem and F. Fernández, Phys. Lett. B **764**, 207 (2017) [arXiv:1606.06148 [hep-ph]].
- [45] Y. Shimizu, D. Suenaga and M. Harada, Phys. Rev. D **93**, no. 11, 114003 (2016) doi:10.1103/PhysRevD.93.114003 [arXiv:1603.02376 [hep-ph]].
- [46] Y. Yamaguchi and E. Santopinto, arXiv:1606.08330 [hep-ph].
- [47] S. Weinberg, Phys. Rev. **130**, 776 (1963).
- [48] F. Aceti and E. Oset, Phys. Rev. D **86**, 014012 (2012) [arXiv:1202.4607 [hep-ph]].
- [49] Q. Wang, X. H. Liu and Q. Zhao, Phys. Rev. D **92**, 034022 (2015) [arXiv:1508.00339 [hep-ph]].
- [50] Q. F. Lü, X. Y. Wang, J. J. Xie, X. R. Chen and Y. B. Dong, Phys. Rev. D **93**, 034009 (2016) [arXiv:1510.06271 [hep-ph]].
- [51] S. H. Kim, H. C. Kim and A. Hosaka, Phys. Lett. B **763**, 358 (2016) [arXiv:1605.02919 [hep-ph]].
- [52] Y. Huang, J. He, H. F. Zhang and X. R. Chen, J. Phys. G **41**, 115004 (2014) [arXiv:1305.4434 [nucl-th]].
- [53] S. H. Kim, H. C. Kim and A. Hosaka, Phys. Rev. D **94**, 094025 (2016) [arXiv:1608.06394 [hep-ph]].